

# Investigation Of Turbulent Mixing Layer With Compressibility Corrections For RANS Models

V. Sharma\*, A. Assam\* and V. Eswaran\*  
Corresponding author: me12m14p000005@iith.ac.in

\* Dept. of Mechanical and Aerospace Engineering, Indian Institute of Technology Hyderabad, India.

**Abstract:** Turbulent mixing is highly affected by fluid compressibility. The current work aims to study the effect of compressibility corrections for 3 different Reynold Averaged Navier Stokes (RANS) turbulence models namely the standard k-epsilon, RNG and Spalart Allmaras models using an in-house parallel three dimensional unstructured CFD solver to compute a high speed mixing layer. The experimental study done by Goebel and Dutton has been used as the benchmark for investigation. The standard k- $\epsilon$  is compared with the RNG model to see the effect of the change in model coefficients on the predicted flow physics. The one equation Spalart Allmaras model is compared with the aforementioned two equation model to make the performance comparison complete. Turbulent quantities like rate of mixing layer growth, turbulence intensity and normalized Reynold's stress have been compared with benchmark results along with mean flow quantities like the self similar velocity profiles and their results have been presented.

*Keywords:* Compressible Flow, RANS models, Turbulence Modeling, Mixing layer, Compressibility Correction.

## 1 Introduction

Mixing streams from flight and exhaust in aerodynamics are of interest in active flow control and propulsion studies. Fluid compressibility modifies the behaviour of turbulence while the strong coupling between momentum and energy significantly alters flow behavior. It has been noted in literature [1] that due to the existence of shock waves attached to coherent structures in the mixing layer, there is unequal pressure dissipation. Although eddy shocklets attached to structures have not been seen in experiments, the footprint of their existence are captured in the study by Hall et al[2]. On the other hand, several DNS studies have witnessed eddy shocklets and their effect[3]. These shocks cause increased dissipation of turbulence not accounted for by the standard Kolmogorov scale dissipation rate. So, it can be concluded that turbulent mixing layers show significant effect of compressibility when experimentally investigated in literature [4, 1, 5, 6]. However comparable numerical modelling of these flows has not been comprehensively addressed, although compressibility corrections[7],[8],[9] have been proposed for RANS turbulence models. A parameter called convective Mach number ( $M_c$ ) has been defined by Bogdanff[4] to quantify the compressibility of a mixing layer and has been used to correlate mixing layer parameters in numerous studies. This and a similar parameter called the relative Mach number  $M_r$ [6], are defined as:

$$M_r = \frac{\Delta U}{\bar{a}} \quad (1)$$

$$M_c = \frac{M_r}{2} \quad (2)$$

where  $\bar{a}$  is the average of free stream speed of sound and  $\Delta U$  is the difference in inlet velocities. In this paper we study the high speed mixing layer. This problem is considered as crucial by the Langley research centre and is mentioned as one of the essential validation benchmark cases for propulsion studies.[10].

## 2 Benchmark Study

The experimental study done by Goebel and Dutton[6] is used as the benchmark for investigation. The apparatus used in the experiments is a channel of size 500 mm x 48 mm x 96 mm, where 500 mm is the length of the viewing section setup for Schlieren photography. A very thin splitter plate of of 2mm length and a thickness of 0.5 mm that separates the two mixing streams confined by top and bottom walls. The local Reynolds number at the exit of the test section, given by:

$$Re_b = \frac{\bar{\rho}\Delta U b}{\mu} \quad (3)$$

Based on Bradshaw results, the  $Re_b$  should be greater than 100,000 for the complete development of the mixing layer allowing similarity solutions. Five cases were examined in the experimental study for  $M_r$  ranging from 0.4 to 1.97. For this paper, we shall address only the results of  $M_r = 0.9$  and 1.73.

## 3 Computational Methodology

### 3.1 Simulation Domain

A domain of size 500 mm x 144 mm x 1 mm is used for simulations as shown in figure 1.

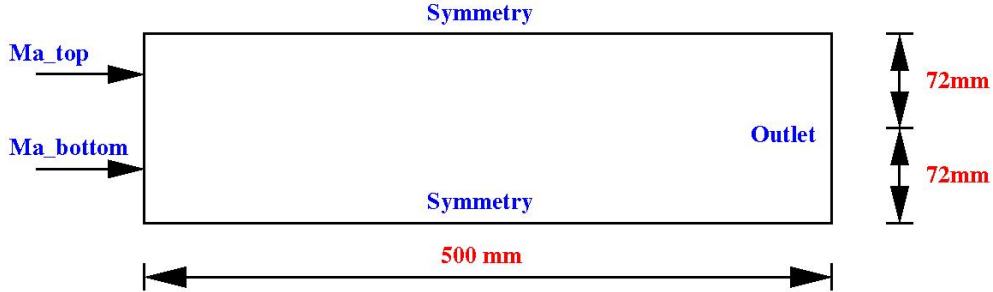


Figure 1: GEOMETRY FOR SIMULATIONS AND ITS BOUNDARY CONDITIONS

We perform two-dimensional simulations, as the benchmark study flow was seen to be two dimensional in nature. Pressure inlet boundary condition has been specified at inlet for the primitive variables (P,  $\mathbf{V}$ , T), whereas dirichlet boundary condition is prescribed for turbulence variables. Pressure outlet boundary condition has been used at the outlet. Top and bottom have been given symmetry boundary conditions as shown in figure 1. We donot model the splitter plate and the confining walls.

### 3.2 Mathematical Modelling

An in-house parallel unstructured three dimensional solver has been developed for solving Navier Stokes equations at all speeds using the algorithm given by Weiss and Smith[11, 12] with explicit time-stepping. Using 2nd order preconditioned Roe scheme[12] with Venkatkrishnan limiter [13] fully turbulent flow is being simulated using the RANS models. The governing equation for the RANS models are given in following subsections:

#### 3.2.1 Standard K- $\epsilon$ model

The governing equation for RANS standard k- $\epsilon$  model as given by Spalding [14] in high Reynolds' number form is implemented as:

$$\frac{\partial}{\partial t}(\rho k) + \frac{\partial}{\partial x_i}(\rho k u_i) = \frac{\partial}{\partial x_j} \left[ \left( \mu + \frac{\mu_t}{\sigma_k} \right) \frac{\partial k}{\partial x_j} \right] + P_k - D_k \quad (4)$$

$$\frac{\partial}{\partial t}(\rho\epsilon) + \frac{\partial}{\partial x_i}(\rho\epsilon u_i) = \frac{\partial}{\partial x_j} \left[ \left( \mu + \frac{\mu_t}{\sigma_\epsilon} \right) \frac{\partial \epsilon}{\partial x_j} \right] + C_{1\epsilon} \frac{\epsilon}{k} P_k - C_{2\epsilon} \rho \frac{\epsilon^2}{k} \quad (5)$$

where:  $\mu_t$ , is computed by combining  $k$  and  $\epsilon$  as follows:

$$\mu_t = \rho C_\mu \frac{k^2}{\epsilon} \quad (6)$$

where  $C_\mu$  is a constant. Turbulent production can be written as :

$$P_k = \tau_{ij} \frac{\partial u_j}{\partial x_i} \quad (7)$$

Linear models use the Boussinesq assumption for modelling the Reynolds' stress  $\tau_{ij}$  as:

$$\tau_{ij} = 2\mu_t \left( S_{ij} - \frac{1}{3} \frac{\partial u_k}{\partial x_k} \delta_{ij} \right) - \frac{2}{3} \rho k \delta_{ij} \quad (8)$$

where  $S_{ij}$  is the strain rate tensor given as:

$$S_{ij} = \frac{1}{2} \left( \frac{\partial u_i}{\partial x_j} + \frac{\partial u_j}{\partial x_i} \right) \quad (9)$$

The constants are:

$$C_{1\epsilon} = 1.44, \quad C_{2\epsilon} = 1.92, \quad C_\mu = 0.09, \quad \sigma_k = 1.0, \quad \sigma_\epsilon = 1.3 \quad (10)$$

### 3.2.2 RNG K- $\epsilon$ Model

The Re-Normalisation Group (RNG) model was proposed by Yakhot et al[15]. In the standard k-epsilon model the turbulent viscosity is determined from a single turbulence length scale, so the calculated turbulent diffusion is that which occurs only at the specified scale, whereas all scales of motion would contribute to the turbulent diffusion. Hence the RNG model to account for the effects of smaller scales of motion. This results in a modified form of the epsilon equation with changes to the production term, equations of  $k$  and  $\epsilon$  remain same as in standard k- $\epsilon$  model, except for change in definition of model constants, as follows:

$$C_{2\epsilon}^* = C_{2\epsilon} + \frac{C_\mu \eta^3 (1 - \eta/\eta_0)}{1 + \beta \eta^3} \quad \eta = Sk/\epsilon, \quad \eta_0 = 4.38, \quad \beta = 0.012, \quad S = (2S_{ij}S_{ij})^{1/2} \quad (11)$$

$$C_{\epsilon 1} = 1.42, \quad C_{\epsilon 2} = 1.68 \quad C_\mu = 0.0845, \quad \sigma_k = 0.7194, \quad \sigma_\epsilon = 0.7194$$

It is interesting to note that the values of all of the constants (except  $\beta$ , which is derived from experiment) are derived explicitly in the RNG procedure.

### 3.2.3 Spalart Allmaras model

The one equation model proposed by Spalart and Allmaras[16] has been implemented in a low-reynolds number form. While several versions of the model exist, has been stated by Allmaras[17] that any form of model is acceptable. Hence, the original form is retained, governing equations for which are as follows:

$$\frac{\partial \tilde{\nu}}{\partial t} + \frac{\partial}{\partial x_i}(\tilde{\nu} u_i) = P_{\tilde{\nu}} - D_{\tilde{\nu}} + \frac{1}{\sigma} \left[ \frac{\partial}{\partial x_i} \left( (\nu + \tilde{\nu}) \frac{\partial \tilde{\nu}}{\partial x_i} \right) + c_{b2} \frac{\partial \tilde{\nu}}{\partial x_j} \frac{\partial \tilde{\nu}}{\partial x_j} \right] \quad (12)$$

where  $P_{\tilde{\nu}}$  is production and  $D_{\tilde{\nu}}$  is destruction of turbulence respectively given by:

$$P_{\tilde{\nu}} = c_{b1} \tilde{S} \tilde{\nu}$$

$$D_{\tilde{\nu}} = c_{w1} f_w \left( \frac{\tilde{\nu}}{d} \right)^2 \quad (13)$$

The turbulent eddy viscosity is computed from:

$$\mu_t = \rho \tilde{\nu} f_{v1} \quad (14)$$

where:

$$f_{v1} = \frac{\chi^3}{\chi^3 + c_{v1}^3}, \quad \chi = \frac{\tilde{\nu}}{\nu} \quad (15)$$

and  $\rho$  is the density,  $\nu = \mu/\rho$  is the molecular kinematic viscosity, and  $\mu$  is the molecular dynamic viscosity. The quantity  $\tilde{S}$  used in the turbulence production term can be written as:

$$\tilde{S} = \Omega + \frac{\tilde{\nu}}{\kappa^2 d^2} f_{v2} \quad (16)$$

where  $\Omega = \sqrt{2W_{ij}W_{ij}}$  is the magnitude of the vorticity,  $d$  is the distance from the field point to the nearest wall.

$$\begin{aligned} f_{v2} &= 1 - \frac{\chi}{1 + \chi f_{v1}} \\ f_w &= g \left[ \frac{1 + c_{w3}^6}{g^6 + c_{w3}^6} \right]^{1/6} \\ g &= r + c_{w2}(r^6 - r), \\ r &= \min \left[ \frac{\tilde{\nu}}{\tilde{S} \kappa^2 d^2}, 10 \right] \\ W_{ij} &= \frac{1}{2} \left( \frac{\partial u_i}{\partial x_j} - \frac{\partial u_j}{\partial x_i} \right) \end{aligned} \quad (17)$$

The constants used are given as follows:

$$\begin{aligned} c_{b1} &= 0.1355, \quad \sigma = 2/3, \quad c_{b2} = 0.622, \quad \kappa = 0.41 \\ c_{w2} &= 0.3, \quad c_{w3} = 2 \\ c_{w1} &= \frac{c_{b1}}{\kappa^2} + \frac{1 + c_{b2}}{\sigma}. \end{aligned} \quad (18)$$

The Boussinesq approximation for modelling the Reynold's stress  $\tau_{ij}$  is given as:

$$\tau_{ij} = 2\mu_t \left( S_{ij} - \frac{1}{3} \frac{\partial u_k}{\partial x_k} \delta_{ij} \right) \quad (19)$$

Since no walls are present in the current case, we set value of  $d$  as  $10^{10}$ , this helps to prevent numerical problems in the solver.

### 3.3 Compressibility Correction

#### 3.3.1 Compressibility Corrections for RNG and Standard K- $\epsilon$ model

In the RANS solution of turbulent flow, the variables are split into a mean and fluctuating part. The mean can be defined as two ways either as the Reynolds average (unweighted average) and Favre averaged (density weighted average). In solving compressible flows, use of Reynolds average introduces correlations involving density fluctuations and modelling of these correlations is difficult. To overcome this a combination of Reynolds and Favre average is used resulting in the following :

$$\frac{\partial}{\partial t}(\rho k) + \frac{\partial}{\partial x_i}(\rho k u_i) = \underbrace{\overline{-\rho u_i'' u_j''}}_{\mathbf{G}} \frac{\partial u_i''}{\partial x_i} - \underbrace{u_i''}_{\mathbf{H}} \frac{\partial P}{\partial x_i} - \underbrace{\overline{\frac{\partial u_i''}{\partial x_i} \sigma''}}_{\mathbf{I}} + \underbrace{\frac{\partial}{\partial x_i} \left[ \overline{-\rho u_j'' (0.5 * u_i'' u_i'')} - \overline{u_i'' \sigma_{ij}''} - \overline{P' u_i''} \right]}_{\mathbf{K}} + \underbrace{P' \frac{\partial u_i''}{\partial x_i}}_{\mathbf{K}} \quad (20)$$

Where a tilde denotes Favre averaged quantities, and a ( $''$ ) denotes fluctuations with respect to Favre mean. An overbar represents a reynolds average and a ( $'$ ) denotes fluctuations with respect to it.  $\overline{\sigma''_{ij}}$  is result of favre averaging, and at low mach numbers it does not represent compressibility effects. The terms resulting from Favre averaging must be modelled in order to close the equation. The terms shown in acpilatl letters represent:

- G : Reynolds Stress modelled as given by equation .
- H : Dilation Dissipation
- I : Rate of dissipation due to molecular effects =  $\rho\epsilon$
- J : Turbulent kinetic energy diffusion due to turbulent fluctuations =  $\frac{\mu_t}{\sigma_k} \frac{\partial K}{\partial x_j}$
- K : Pressure Dilatation.

It has been noted in literature [1] that due to the existance of shock waves attached to coherent structures in the mixing layer, there is unequal pressure dissipation. Although eddy shocklets attached to structures have not been seen in experiments, several DNS studies have witnessed eddy shocklets and their effect[3].

These shocks cause increased dissipation of turbulence not accounted for the by standard Kolmogorov scale dissipation rate. Researchers have proposed to model the effect as an additional dissipation rate, the term  $Y_m$ , which has been implemented in the solver. This term includes additional effects of pressure dilation  $\mathbf{K}$  and is modelled as proposed by Sarkar[18]. To close the term  $\mathbf{H}$  in equation 20, the evaluation of turbulent fluctuations on an acoustic time scale is considered. They consider the effect of varying compressibility on rate of dissipation of turbulent kinetic energy ( $\epsilon$ ), hence a model was proposed:

$$Y_M = 2\rho\epsilon M_t^2 \quad (21)$$

where  $M_t$  is defined in equation 22.

$$M_t = \sqrt{\frac{k}{a^2}} \quad (22)$$

The term  $\mathbf{K}$  appears due to the non divergent fluctuating velocity field. Pressure dilatation refers to work done due to simultaneous fluctuations in density corresponding to fluctatons in pressure. Sarkar et al.[8] conducted an analysis of the density correlation in both decaying compressible turbulence and homogeneous shear turbulence and proposed the following model:

$$Y_P = -\alpha_3 P_k M_t^2 + \alpha_4 \rho \epsilon M_t^2 \quad (23)$$

where  $\alpha_3 = 0.4$  and  $\alpha_4 = 0.2$ .

### 3.3.2 Compressibility Corrections for Spalart Allmaras model

Due to the absence of the turbulent mach number in the equations of the Spalart Allmaras model,the compressibility correction employed in 2-equation models cannot be used. So, instead, Paciorri and Sabetta [9], suggested corrections that relate mixing layer thickness to turbulent viscosity using the experimental correlation between growth rate and thickness of mixing layer.This is analogous to having dependence on turbulent mach number, but actually imposes direct dependence on the convective mach number. The compressibility correction is hence modeled as:

$$Y_C = -C_c \frac{\tilde{v}^2}{a^2} \frac{\partial U_i}{\partial x_i} \frac{\partial U_i}{\partial x_i} \quad (24)$$

where  $C_c$  is constant and its value is determined as 3.5. This term is then added to transport equation.

## 3.4 Grid Independence Study

The mesh was created using ICCFD software. The hyperbolic mesh distribution law is used for nodes in the Y direction, so there are more nodes in the mixing layer and around 80% of the nodes within 24mm frWSom

centre for both inlets, as shown in fig 1.

Grid convergence index (GCI) [19] has been used to establish the order of accuracy on the desired grid. Three sets of grids have been used for study as shown in Table 1. We use standarad k- $\epsilon$  model without any compressibilty correction for the grid convergence study.

Name	Size	Elements
h1	121x111	13200
h2	91x86	7650
h3	68x68	4489

Table 1: Table showing nodes distribution and number of elements

The non dimensional growth rate of thickness  $\phi = \frac{db}{dx}$  is taken as the parameter for which the GCI study is done. It should be noted, that  $\phi$  has been computed without any compressibility correction. The results of the study have been presented in the Table 2. We define the variables with respect to h1 mesh as follows: Refinement ratio can be defined as:

Parameter	Value
$N_1, N_2, N_3$	13200, 7650, 4489
$r_{21}$	1.31
$r_{32}$	1.31
$\phi_1$	0.09612
$\phi_2$	0.09897
$\phi_3$	0.09971
p	5.06
$\phi_{ext}^{21}$	0.09996
$e_a^{21}$	0.742%
$e_{ext}^{21}$	0.259%
$GCI^{21}$	0.241%
$e_a^{32}$	0.909%
$e_{ext}^{32}$	2.78%
$GCI^{32}$	0.934%

Table 2: Table showing grid convergence index study

$$r_{21} = \sqrt{\frac{N_1}{N_2}} \quad (25)$$

where  $N_1$  is number of elements in h1 mesh, and so forth. Refinement ratio has been kept as 1.31 as seen in 2. Richardson extrapolation gives a value ( $\phi_{ext}^{21}$ ) of 0.09996 for the finest mesh(h1) . Numerical uncertainty for h2 mesh can be reported as  $GCI^{32} = 0.943\%$ , and extrapolated relative error( $e_{ext}^{32}$ ) of 2.78 % , and hence the h2 grid has been used for the study.

### 3.5 Validation

The solver has been validated for several benchmark problems[11]. Validation has been done against the benchmark study of Goebel and Dutton data for  $M_r = 1.73$  [6], for the conditions also described in Table 3. Parameters and variables that have been used are defined:

$$\Delta u = u_1 - u_2 \quad (26)$$

$$y_1 = u_1 - 0.1\Delta u \quad (27)$$

$$y_2 = u_2 + 0.1\Delta u \quad (28)$$

$$b = y_1 - y_2 \quad (29)$$

$$y_0 = (y_1 + y_2) * 0.5 \quad (30)$$

$$y_{norm} = \text{frac}(y - y_0)b \quad (31)$$

$$u_{norm} = (u - u_2)/(u_1 - u_2) \quad (32)$$

Once the mixing layer is fully developed, the velocity profiles can be expressed in self-similar form. The regions of mixing layer where the mean velocity is considered to be self-similar are listed in [6]. For  $M_r = 1.73$ , the region is from 100 mm to 150 mm in the streamwise direction. As we do-not model the splitter plate, we plot the values of  $u_{norm}$  against  $y_{norm}$  in this region to check if in this region, self similarity has been attained. Again, the standard k- $\epsilon$  model has been used without any compressibility correction for the results presented in this section. Figure 2a shows that the self-similarity has been successfully captured in the region

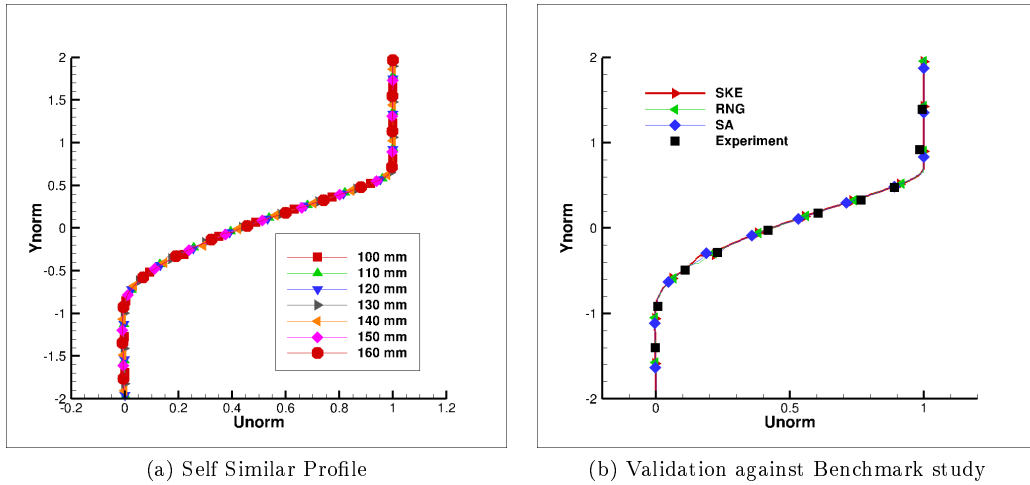


Figure 2: Profile of normalized velocity plotted against normalized length in y direction

described by benchmark study, hence modelling of splitter plate is apparently not necessary. Self similar velocity profile obtained from all three models without any compressibility correction is then plotted against the experimental data [6] and an excellent match is obtained as seen in Figure 2b.

## 4 Results

In this paper, we have present only the results of  $M_r = 0.9$  and  $1.73$  of benchmark study with standarad k- $\epsilon$ , RNG and Spalart Allmaras models. The inlet conditions for both the cases has been presented in Table 3. Since, pressure inlet boundary condition has been used, static pressure, total temperature and tubulence intensity(TI) as given in bench mark study have been shown .

To calculate values of turbulence variable at the inlet, we require length scale, which has been calculated using the formula:

$$l = 0.007L. \quad (33)$$

Table 3: PARAMETERS FOR INLET BOUNDARY CONDITIONS

$M_r = 0.9$				
<i>Section</i>	<i>Ma</i>	$P_{static}(Pa)$	$T_{total}(K)$	<i>TI</i>
<i>Top</i>	1.91	49000	578	0.0114
<i>Bottom</i>	1.35	49000	295	0.10117
$M_r = 1.73$				
<i>Top</i>	2.35	36000	390	0.0114
<i>Bottom</i>	0.36	36000	282	0.10117

Where  $L$  has been taken as 24 mm for each inlet as given in the experimental benchmark study. Using the following formula, we calculate the values of turbulent kinetic energy ( $k$ ) and turbulence dissipation ( $\epsilon$ ) at inlet, with a turbulence intensity(TI) of 1.114% for the top inlet and 10.117% for the bottom inlet, as stated in experiments. The turbulent kinetic energy and its dissipation rate determined at the inlet as:

$$k = \frac{3}{2} (U_{mean} I)^2 \quad (34)$$

$$\epsilon = C_{\mu}^{\frac{3}{4}} \frac{k^{\frac{3}{2}}}{l} \quad (35)$$

Similarly, the eddy viscosity has been calculated as:

$$\nu = \sqrt{1.5} \frac{(U_{mean} l)}{2} \quad (36)$$

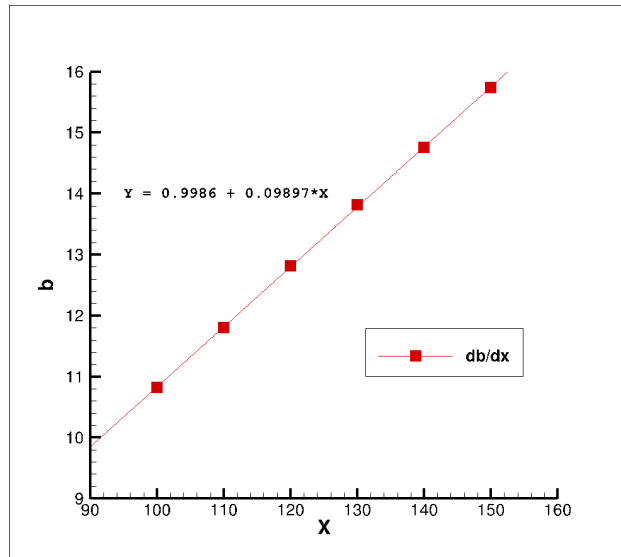


Figure 3: Mixing layer thickness for  $Mr = 1.73$  without any compressibility correction

#### 4.1 Case 1 $M_r = 1.73$

The mixing layer thickness is calculated, as given in Goebel and Dutton[6].By equation 29, we plot mixing layer thickness against streamwise direction in figure 3 for  $M_r = 1.73$ . Using a linear fit, we obtain the growth rate for the case under investigation with relative Mach number of 1.73

Growth rates obtained from standard k-epsilon (SKE), RNG and Spalart Allmaras (SA) models without any compressibility correction are given in Table 4.

Model	Growth Rate
SKE	0.09897
RNG	0.09893
SA	0.09888
Experiment	0.05

Table 4: Growth rates compared of RANS models with Benchmark study

The computed growth rates for all three models are very close, but are around twice in the experimental study, although the self-similar velocity profiles had an excellent match as seen in figure 2b. It can be suspected that fluid compressibility has modified the behaviour of turbulence while the strong coupling between momentum and energy has significantly altered flow behavior, as compared with incompressible mixing layer.

Hence the flow is simulated with the compressibility corrections for the standard k- $\epsilon$  model as described in Section 3.3.1. Flow is computed with the dilation dissipation compressibility correction proposed by Sarkar [7],but without the acoustic scale correction and this shall be referred to as **caseA**.

Then the effects of acoustic scales in flow are modelled using pressure dissipation compressibility correction as proposed by Sarkar [8]. This is referred to as **caseB**. This results in the rate of mixing layer growth as 0.06013 for SKE model, which is a significant reduction as compared to case A, but is around 20% more than experimental value. Then the , RNG model is simulated with case B and rate of growth of mixing layer is further reduced to 0.05481. For the Spalart Allmaras model, the effect of compressibility is modelled using correction suggested by Piccori and Sabetta [9] as described in section 3.3.2. This is referred as **caseC**. The results have been tabulated in Table 5.

Model	Without Correction	Case A	Case B	Case C
SKE	0.09897	0.06965	0.06013	-
RNG	0.09893	-	0.05481	-
SA	0.09888	-	-	0.05118

Table 5: Growth rates compared of RANS models

The experimental growth rate was seen to be 0.05, as evident from Table 5, the best result is obtained with the Spalart Allmaras model, and closely by RNG model. The Reynolds' stress using Equation 37 and the turbulence intensity using Eq.34 has also been plotted in Figure 5.

$$\tau_{ij,norm} = \frac{\tau_{ij}}{\Delta u^2} \quad (37)$$

#### 4.2 Case 2 $M_r = 0.9$

Similarly, we compare the predictions of the growth mixing layer for  $M_r = 0.9$ . Now using case B of the standard k- $\epsilon$  and RNG model and case C for the Spalart Allmaras model, it is seen that the compressibility corrections give better results for turbulence intensities but worse for Reynolds' stresses.

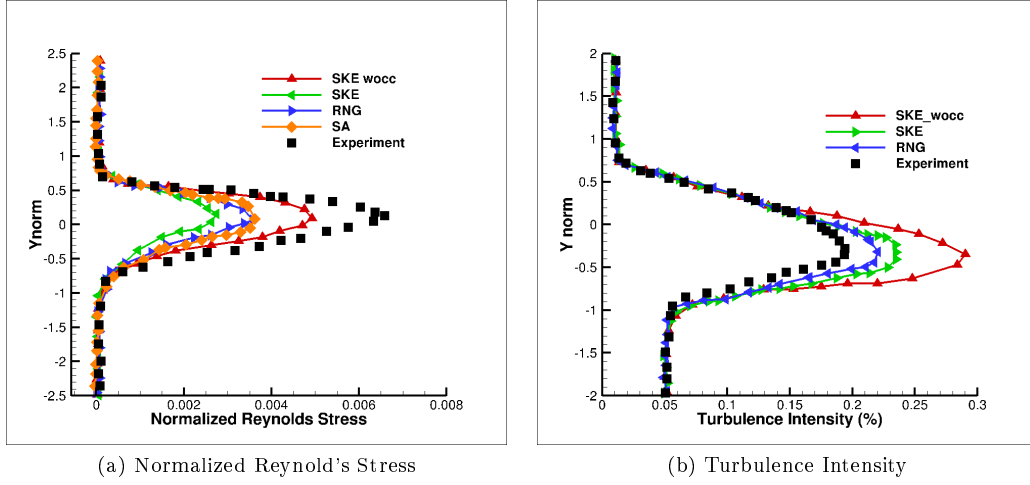


Figure 4: Comparison of turbulent quantities from RANS models against experimental data for  $Mr = 1.73$

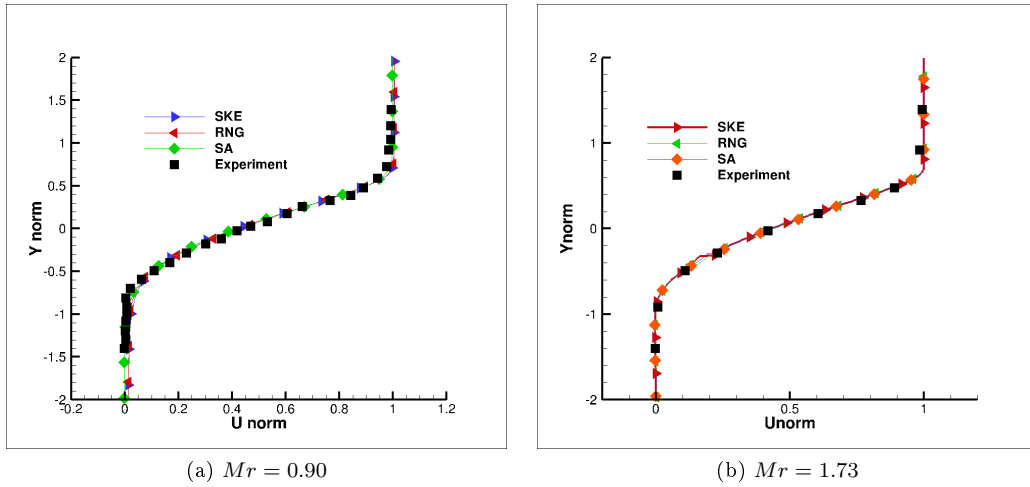


Figure 5: Case B comparison of self similar velocities from RANS models against experimental data

Rate of growth of mixing layer thickness has been computed and presented in table 6. Turbulence quantities for  $Mr = 0.9$  have been plotted in figure 6.

Model	Growth Rate
SKE	0.03577
RNG	0.03591
SA	0.03506
Experiment	0.038

Table 6: Growth rates with compressibility corrections of RANS models

It is observed that including compressibility corrections enhance the prediction of the mixing layer growth rate considerably, but the Reynolds' stress and turbulence intensity predictions do not match the experiment's

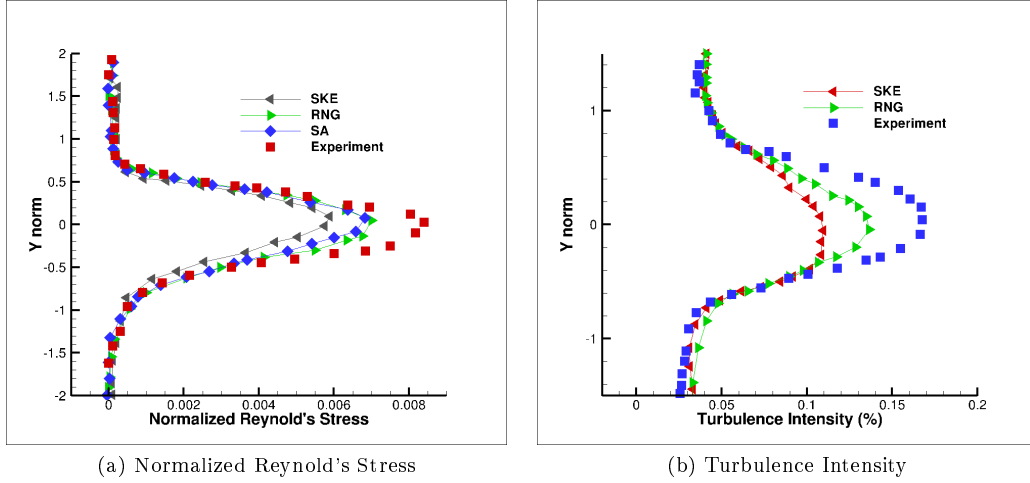


Figure 6: Comparison of turbulent quantities from RANS models with compressibility corrections against experimental data for  $Mr = 0.9$

results.

## 5 Conclusion

In the present work, an in-house three dimensional unstructured grid solver with turbulence modeling capabilities[11] was used to study a high speed mixing layer with  $Mr = 0.9$  and  $Mr = 1.73$ . The experimental study by Goebel and Dutton[6] was used as benchmark. Grid with 7650 elements was selected through a grid convergence study as shown in section 3.4.

The self similar profiles of velocity obtained from the solver give an excellent match with experiments, even without any compressibility corrections. However, turbulent quantities such as rate of growth of mixing layer thickness, normalized Reynold's stress and turbulence intensity should also be compared with benchmark cases, in order to get a clear picture of performance of a turbulence model. Hence model specific compressibility corrections were implemented. As seen in section 4, standard k- $\epsilon$  model is out performed by RNG and Spalart Allmaras model in predicting turbulent quantities for  $Mr = 1.73$ . It is also seen that such high convective Mach number flows cannot be modelled without modelling acoustic scales of turbulence.

For  $Mr = 1.73$ , all models over predict the growth rate by nearly 100%, without any compressibility correction. As seen in Table 5, rate of mixing layer growth when dilation dissipation and pressure dilataion corrections are introduced is 0.06013 for SKE and 0.05481 for RNG model. Spalart Allmaras model with its single compressibility correction results in a growth rate of 0.05118, which is quite close to experimental value, a difference of just nearly 2%. All RANS models under-predict normalized Reynolds' stress and over-predict turbulence intensity as compared to the experimental study, which can be attributed to difference in results with growth of mixing layer.

However, for  $Mr = 0.9$ , growth rate obtained with respective compressibility corrections from standard k- $\epsilon$  model is around 6.23% from experimental value of around 0.038. For RNG, this difference reduces to around 5.28%, and for Spalart Allmaras model, it is to be around 8.34%. All the models over predict normalized reynold's stress and under predict turbulence intensity as compared to experimenrs study, hence the rate of mixing layer growth is under-predicted.

To conclude, compressibility corrections are very important for the turbulent modelling of high speed mixing layers with high relative mach numbers. But their impact is reduced for lower relative mach nummer

## 6 Acknowledgement

The authors gratefully acknowledge Dr. Debasis Chakraborty(CFD Division, DRDL Hyderabad) for his invaluable insights and opinions on the problem statement.

## References

- [1] Dimitri Papamoschou and Anatol Roshko. The compressible turbulent shear layer: an experimental study. *Journal of fluid Mechanics*, 197:453–477, 1988.
- [2] JL Hall, PE Dimotakis, and H Rosemann. Experiments in nonreacting compressible shear layers. *AIAA journal*, 31(12):2247–2254, 1993.
- [3] John Papp and K Ghia. Study of turbulent compressible mixing layers using two-equation turbulence models including an rng k-epsilon model. In *36th AIAA Aerospace Sciences Meeting and Exhibit*, page 320, 1998.
- [4] DW Bogdanoff. Compressibility effects in turbulent shear layers. *AIAA journal*, 21(6):926–927, 1983.
- [5] MR Gruber, AS Nejad, TH Chen, and JC Dutton. Mixing and penetration studies of sonic jets in a mach 2 freestream. *Journal of Propulsion and Power*, 11(2):315–323, 1995.
- [6] Steveng Goebel and Jcraig Dutton. Experimental study of compressible turbulent mixing layers. *AIAA journal*, 29(4):538–546, 1991.
- [7] Sutanu Sarkar, Gordon Erlebacher, M Yousuff Hussaini, and Heinz Otto Kreiss. The analysis and modelling of dilatational terms in compressible turbulence. *Journal of Fluid Mechanics*, 227:473–493, 1991.
- [8] S Sarkar. The pressure–dilatation correlation in compressible flows. *Physics of Fluids A: Fluid Dynamics*, 4(12):2674–2682, 1992.
- [9] Renato Paciorri and Filippo Sabetta. Compressibility correction for the spalart-allmaras model in free-shear flows. *Journal of Spacecraft and Rockets*, 40(3):326–331, 2003.
- [10] Langley Research Centre. Nasa’s 40
- [11] Vatsalya Sharma, Ashwani Assam, and Vinayak Eswaran. Development of all speed three dimensional computational fluid dynamics solver for unstructured grids. *6th International and 43rd National Conference on Fluid Mechanics and Fluid Power*, 2016.
- [12] Jonathan M Weiss and Wayne A Smith. Preconditioning applied to variable and constant density flows. *AIAA journal*, 33(11):2050–2057, 1995.
- [13] V Venkatakrisnan. 'on the accuracy of limiters and convergence to steady state solutions,' aiaa paper 93-0880, jan. 1993.
- [14] Dudley Brian Spalding. Mathematical models of turbulent flames; a review. *Combustion Science and Technology*, 13(1-6):3–25, 1976.
- [15] VSASTBCG Yakhot, SA Orszag, S Thangam, TB Gatski, and CG Speziale. Development of turbulence models for shear flows by a double expansion technique. *Physics of Fluids A: Fluid Dynamics*, 4(7):1510–1520, 1992.
- [16] PRaA Spalart and S1 Allmaras. A one-equation turbulence model for aerodynamic flows. In *30th aerospace sciences meeting and exhibit*, page 439, 1992.
- [17] Steven R Allmaras and Forrester T Johnson. Modifications and clarifications for the implementation of the spalart-allmaras turbulence model. In *Seventh international conference on computational fluid dynamics (ICCFD7)*, pages 1–11, 2012.
- [18] S Sarkar and B Lakshmanan. Application of a reynolds stress turbulence model to the compressible shear layer. *AIAA journal*, 29(5):743–749, 1991.
- [19] Ishmail B Celik, Urmila Ghia, Patrick J Roache, et al. Procedure for estimation and reporting of uncertainty due to discretization in {CFD} applications. *Journal of fluids {Engineering-Transactions} of the {ASME}*, 130(7), 2008.